Calorimetric study on interaction of dioxygen with alumina supported palladium

Yung-Shen Ho [1], Chen-Bin Wang, Chuin-Tih Yeh [*]

Department of Chemistry, National Tsinghua University, Hsinchu 30043, Taiwan, ROC

Abstract

Pd/Al$_2$O$_3$ samples of various palladium loadings were prepared with the incipient-wetness method. With an increase in the palladium loading, the average diameter (d) of palladium crystallites on these samples was estimated from chemisorption of hydrogen to vary from 10 to 80 Å. Also, the phenomena of oxidizing these dispersed palladium crystallites with dioxygen were studied by a simultaneous TG-DSC instrument. The extent of oxidation was found to increase in three steps with temperature: adsorption on the surface of Pd crystallites at ambient or lower temperatures, penetration of oxygen into the sublayer when raising the temperature over 300 K, and formation of palladium oxide structure at 800 K. The heat evolved during oxygen adsorption on palladium crystallites depended on their average diameter (d) and displayed a relationship of $-Q_{ad}$ [kJ (mol O$_2$)$^{-1}$] = 373 $-$ 14d (nm). Evolved heat upon palladium oxidation decreased with the extent of oxidation (N_O/N_{Pd} ratio in the product). Upon the complete oxidation at 800 K, a diameter independent $\Delta_f H^{\circ}_{298}$(PdO) of $-$187 $\pm$ 2 kJ (mol O$_2$)$^{-1}$ was subsequently obtained. This value differs significantly from the literature $\Delta_f H^{\circ}_{298}$(PdO) values ($-$220 kJ (mol O$_2$)$^{-1}$) obtained from the Clausius–Clapeyron equation. The discrepancy should have resulted from a partial desorption of oxygen from PdO during measurement.

Keywords: Calorimetry; Heat of adsorption; Heat of oxidation; Enthalpy of PdO formation; Phenomena of oxidation

1. Introduction

Supported palladium was recently found in our laboratory to be an active catalyst in the thermal decomposition of NO into N$_2$ and O$_2$. In the presence of Pd/Al$_2$O$_3$ catalysts, the N$_2$ conversion of this catalyzed reaction was satisfactorily high (80%) at 1173 K. Unfortunately,

the catalytic activity decreased with the reaction temperature because a substantial energy barrier existed in the desorption of oxygen from palladium surface [1]. Understanding the thermodynamic and kinetic properties of the following adsorption–desorption reaction therefore became essential in reducing the required temperature for the NO decomposition:

$$2Pd + O_2 \rightleftharpoons 2PdO. \qquad (1)$$

Interaction between dioxygen and palladium surface has been extensively studied [2–4]. The following three oxygen species have been found

* Corresponding author.
[1] Present address: Refining & Manufacturing Research Center, Chinese Petroleum Corporation, Chayi, Taiwan, ROC.

from the thermal desorption spectroscopy of oxidized samples:

1. Molecularly adsorbed dioxygen: this species was formed when exposing palladium surface to dioxygen at low temperatures and later was desorbed in first-order kinetics from the surface on raising the system temperature over 160 K.

2. Atomically adsorbed oxygen: this species was formed from dioxygen–palladium interaction at $T_{ad} > 150$ K and later manifested a second-order kinetics desorption near 900 K.

3. Incorporated oxygen ions: the species resulted from the penetration of oxygen ions into bulk palladium upon oxidation at $T > 400$ K and desorbed at $T \geq 1000$ K.

The enthalpy of PdO formation $(\Delta_f H)$ presents the heat evolved upon oxidation of palladium metal by dioxygen into palladium oxide. The $\Delta_f H^\circ_{298}$ has been measured to be -220 ± 12 kJ $(\text{mol } O_2)^{-1}$ (Table 1) through the Clausius–Clapeyron equation by monitoring the temperature profile of oxygen vapor pressure over palladium oxide.

The heat evolved upon adsorption of oxygen on palladium surface $(-Q_{ad})$ varied from 170 to 330 kJ $(\text{mol } O_2)^{-1}$ for foil and film samples (Table 2). In combined volumetric (for measuring the amount of oxygen uptake) and calorimetric (for measuring the heat evolved during the uptake) studies, the $-Q_{ad}$ of the oxygen

Table 1
Previously reported heat of PdO formation at 298 K from the dissociation of PdO

Author	Method	$\Delta_f H^\circ_{298}$ [kJ (mol $O_2)^{-1}$]	Ref.
Wohler	C–C equation [a]	−217	[5]
Schenck and Kurzen	C–C equation [a]	−217	[6]
Wohler and Jockum	calorimetric	−171	[7]
Bell et al.	C–C equation [a]	−224	[8]
Bayer and Wiedemann	C–C equation [a]	−229	[9]
Brewer	calorimetric	−176	[10]
Value in encyclopedia		−245 ± 84	[11]
Value in encyclopedia		−171	[12]

[a] Calculated by the Clausius–Clapeyron equation.

Table 2
Previously reported heat of adsorption of oxygen on palladium

Sample	Technique	$-Q_{ad}$ [kJ (mol $O_2)^{-1}$]	Ref.
Pd(111)	TPD	230	[13]
Pd(100)	isotherm	251	[14]
Pd(110)	isotherm	334 → 201 [a]	[15]
Pd black	isotherm	201	[16]
Pd film	calorimetry	280	[17]
Pd wire	TPD	234	[18]
Pd/MgO	calorimetry	334 → 167 [b]	[19]
Pd powder	calorimetry	222	[20]
Pd/SiO$_2$	calorimetry	293 → 209 [b]	[20]
Pd/Al$_2$O$_3$	calorimetry	334 → 209 [b]	[20]
Pd/SiO$_2$–Al$_2$O$_3$	calorimetry	251 → 188 [b]	[20]
Pd/TiO$_2$	calorimetry	326 → 259 [b]	[20]

[a] The range indicates that the differential enthalpy changes with the coverage (θ). The large value denotes the enthalpy measured at low θ.
[b] The range indicates that the integral enthalpy changes with the average diameter of palladium crystallites (d). The large value represents the enthalpy measured from a sample with the smallest d.

adsorption on supported palladium catalysts was varied with the particle size of palladium crystallites [19,20]. $-Q_{ad}$ was around 200 kJ (mol $O_2)^{-1}$ when the average diameter (d) was larger than 3.0 nm but increased to 320 kJ (mol $O_2)^{-1}$ when decreasing d.

In this investigation, a simultaneous TG-DSC technique is employed to measure the $-Q_{ox}$ (heat of oxidation, including $-Q_{ad}$ and $-\Delta_f H$) values of oxidizing palladium crystallites supported on alumina by dioxygen. Particular emphasis is placed on the variation of $-Q_{ox}$ with the extent of oxidation.

2. Experimental

Pd/Al$_2$O$_3$ samples of various palladium loadings were prepared by the incipient-wetness method through impregnating γ-Al$_2$O$_3$ (Merck, surface area = 108 m^2/g) with H$_2$PdCl$_4$ solutions. Obtained slurries were pretreated consecutively with an overnight drying at 383 K and a 4 h calcination at 773 K before storing as

testing samples. The palladium loading on these samples was determined by Perkin-Elmer 5000 atomic absorption spectroscopy.

The dispersion (fraction of exposed atoms) of palladium on these samples was determined by chemisorption of hydrogen at room temperature. Fig. 1 presents the variation in the isotherm of hydrogen adsorption with the palladium loadings. The dispersion (D) of each sample was estimated from the N_H^m/N_{Pd} uptake at $P_{H_2} = 10$ Torr and is revealed in Table 3 to have decreased from 90% to 14% when increasing the palladium loading. Also, oxygen uptake (N_O/N_{Pd}) and $-Q_{ox}$ values during oxidation by dioxygen were obtained from a commercial Setaram TG-DSC 111 calorimeter. This instrument is a dual port calorimeter permitting evacuation treatments at a vacuum pressure of 5×10^{-1} Torr as well as a simultaneous TG (thermogravimetry) and DSC (differential scanning calorimetry) measurement in the temperature range between ambient temperature and 800 K. The TG and the DSC have a sensitivity of 0.25 μg and 10 μw, respectively. Pure support was mounted in the reference port as a blank to cancel the potential changes in Δm and ΔH due to physical adsorption of purging gas on the support.
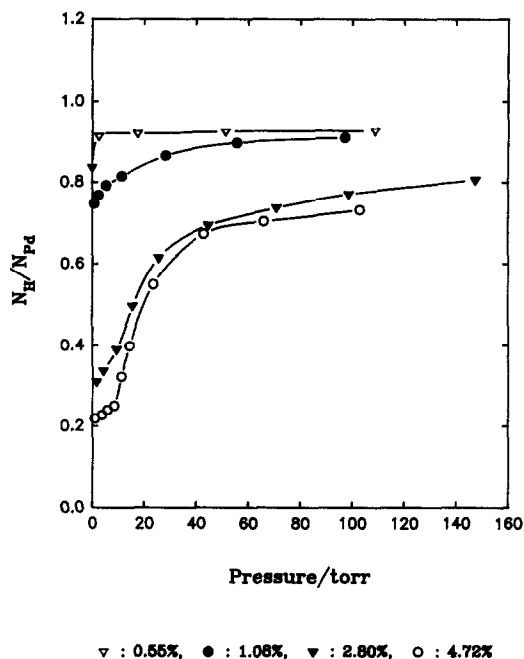

▽ : 0.55%, ● : 1.08%, ▼ : 2.80%, ○ : 4.72%

Fig. 1. Isotherms for hydrogen chemisorption on Pd/Al$_2$O$_3$ samples with various palladium loadings at 300 K (▽: 0.55%; ●: 1.08%; ▼: 2.80%; ○: 4.72%). The dispersion of palladium on each sample may be estimated from the uptake N_H / N_{Pd} at $P_{H_2} = 5$ Torr.

Each testing sample was preheated from RT to 573 K at a rate of 10 K/min in an Ar flow of 30 ml min^{-1}. After the temperature reached 573 K, an 1 h pulse of 10 ml min^{-1} H$_2$ was added

Table 3
Heats of O$_2$ adsorption and enthalpy of PdO formation on Pd/Al$_2$O$_3$

Sample	Hydrogen chemisorption		Oxygen adsorption		Formation of palladium oxide		N_O^{ad}/N_H^m
	D (N_H^m/N_{Pd})	d (nm)	N_O^{ad}/N_{Pd}	Q_{ad} [kJ (mol O$_2$)$^{-1}$]	N_O^b/N_{Pd}	$\Delta_f H$ [kJ (mol O$_2$)$^{-1}$]	
10.09% Pd	0.14	7.9	0.10	−253	0.93	−188	0.71
4.72% Pd	0.21	5.2	0.14	−293	1.05	−184	0.67
2.80% Pd	0.30	3.7	0.21	−330	1.04	−188	0.70
2.04% Pd	0.25	4.4	0.19	−326	0.96	−184	0.76
1.07% Pd	0.52	2.1	0.33	−334	1.01	−188	0.63
1.08% Pd	0.80	1.4	0.48	−346	1.24	−185	0.60
0.55% Pd	0.91	1.2	0.35	−359	1.32	−173	0.38
						−186 ± 2 [a]	0.68 ± 0.05 [a]

N_H^m: Monolayer uptake of hydrogen atoms from H$_2$ chemisorption at $P_{H_2} = 10$ Torr and $T = 298$ K.
d: Average diameter of palladium crystallites calculated from $1.1/(N_H^m/N_{Pd})$.
N_O^{ad}: Uptake of oxygen atoms at 298 K.
N_O^b: Uptake of oxygen atoms at 773 K.
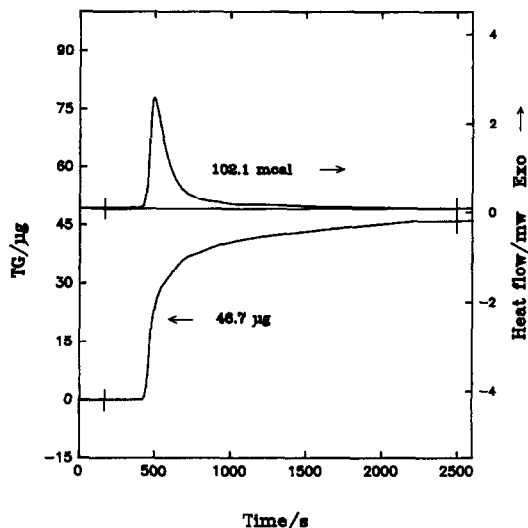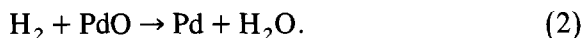[a] Average value from the first six samples in this table.

Fig. 2. The TG-DSC diagram obtained from oxidation of 50 mg 4.72% Pd/Al$_2$O$_3$ sample with dioxygen at 298 K.

from an auxiliary inlet into the Ar flow to reduce the sample according to the chemical equation

$$H_2 + PdO \rightarrow Pd + H_2O. \qquad (2)$$

A loss in sample weight and an evolution of heat were simultaneously observed by the calorimeter due to this reduction. After terminating the H$_2$ flow, the sample temperature was subsequently raised further to 723 K in the Ar flow. After a 2 h desorption of adsorbed hydrogen at 723 K (by evacuating to a vacuum of ca. 5×10^{-1} Torr), the reduced sample was automatically cooled in the Ar flow to a predetermined oxidizing temperature (T_{ox}) and oxidized by a flow of 10 ml min^{-1} O$_2$, introduced from the auxiliary inlet into the Ar flow. Reaction (1) could be detected by the calorimeter from a gain in weight as well as a simultaneous evolution of heat ($-Q_{ox}$).

Fig. 2 presents a TG-DSC time profile on oxidizing 50 mg 4.72%Pd/Al$_2$O$_3$ with dioxygen at 298 K. The oxidation rate decreased with the reaction time with $\Delta m = 46.8$ μg and $-Q_{ox} = 102.1$ mcal after 2×10^3 s of reaction. The oxygen uptake in each oxidation, N_O, was determined according to the Δm obtained after 2×10^3 s of reaction.

3. Results and discussion

3.1. Gravimetric study

Fig. 3 presents the temperature profile of ratio N_O/N_{Pd} observed for three samples with different palladium loadings. Each temperature profile in Fig. 3 can be distinguished into three stages:

1. The N_O/N_{Pd} ratio remained more or less at a constant plain value at $T < 300$ K;
2. The ratio gradually increased from the plain value to a plateau value between 300 and 800 K;
3. The ratio remained at the plateau value after $T > 800$ K.

The three stages are tentatively assigned as chemisorption of oxygen on the surface of palladium crystallites, penetration of oxygen into sublayers, and termination of the oxidation, respectively. The limitation to surface oxidation at low temperatures would imply that penetration
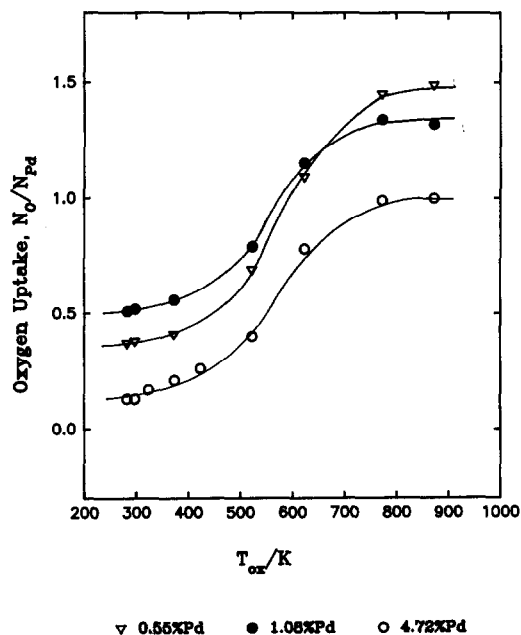

Fig. 3. Temperature profiles of oxygen uptake on various Pd/Al$_2$O$_3$ samples (▽: 0.55%; ●: 1.08%; O: 4.72%).

Table 4
The chemical stoichiometry reported in the literature for adsorption of oxygen on palladium at 300 K

Sample	Method	N_O^{ad}/N_H^m	Ref.
Pd film	volumetric	0.70	[17]
Pd powder	flow	0.66	[21]
Pd/SiO$_2$	volumetric	0.68	[22]
Pd/Al$_2$O$_3$	volumetric	0.60	[23]
Pd powder	gravimetric	0.65	[24]

of oxide ions into sublayers of palladium has an energy barrier and the thermal agitation of the surface ions was not sufficient for the diffusion. However, the penetration process in our palladium crystallites (less than 100 Å initiated at a temperature of 300 K, which is much lower than that (400 K) is reported for samples of palladium foil (or film) [2,3]. The loose texture of our tiny palladium crystallites ($d < 100$ Å) likely had a lower energy barrier for the penetration of oxygen anions than their well packed crystallines ($d \sim 1000$ Å).

Table 3 compares the N_O/N_{Pd} ratio obtained at various oxidation stages. The chemisorption-stage ratio, as expected, generally increased with the dispersion of palladium on the sample (except the 0.55% Pd/Al$_2$O$_3$). In the last column of Table 3, a comparison was made between the oxygen uptake at the adsorption stage (N_O^{ad}) with the monolayer hydrogen uptake (N_H^m). The N_O^{ad}/N_H^m ratio was found to be 0.68 ± 0.05. The ratio correlates sufficiently with ratios reported in the literature (Table 4) for various palladium samples at 300 K.

The extent of palladium oxidation generally increased with temperature. Upon oxidation at 800 K, the N_O/N_{Pd} ratio obtained reached a maximum value of 1.0 (indicating PdO stoichiometry) when the dispersion was low ($D < 60\%$). Formation of bulk PdO is therefore indicated by the forward reaction of Eq. (1). The ratio increased to a value larger than 1.0 when the average diameter of palladium crystallites was less than 2.0 nm ($D > 60\%$). A partial formation of PdO$_2$, i.e.,

$$Pd + O_2 \rightarrow PdO_2, \qquad (3)$$

became evident on oxidation of these highly dispersed samples.

PdO is the only oxide form of palladium that can be found in handbooks [12]. In the previous available literature [25], PdO$_2$ crystallines have only been successfully synthesized at a high O$_2$ pressure (35–40 bar) from fusion of PdO with KClO$_3$. The PdO$_2$ sample synthesized under this condition was thermally stable at an ambient environment but decomposed into PdO when raising the temperature over 343 K. Our gravimetric result therefore indicated that a small-sized PdO$_2$ would enhance thermal stability and thereby become an alternate product from oxidation of a well dispersed palladium. Interestingly, a similar size-dependent result has already been suggested in the literature for platinum oxide when oxidizing supported platinum (i.e., a closely related noble metal) with dioxygen [26].

Fig. 4 presents the time profile of the fraction of oxygen uptake ($f = \Delta m_t / \Delta m$, where Δm_t and Δm denote the weight gain after an oxidation time t and after 2×10^3 s of oxidation,
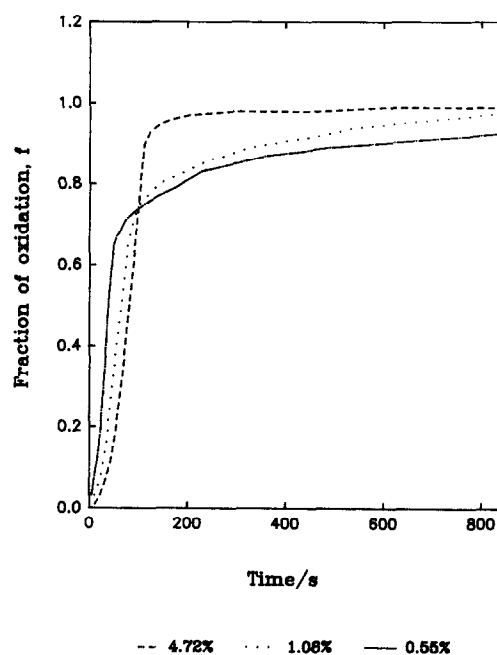

Fig. 4. Time profiles for the fraction ($f = \Delta m_t / \Delta m$) of palladium oxidation at 773 K (– · –: 0.55%; · · · ·: 1.08%; – – –: 4.72%).

respectively) during oxidation at 773 K. A sub-stantial decrease in the oxidation rate of the two samples with a palladium loading of 1% or less was found after $f > 0.7$. The slowing-down in the oxidation rate was attributed primarily to the oxidation of finely dispersed palladium atoms which fell into the empty cavity of the octahe-dral site of alumina, i.e.,

$$2Pd_h + O_2 \rightarrow 2Pd_hO, \tag{4}$$

where Pd_h denotes palladium atoms in the holes of the Al_2O_3 structure. A good portion of palla-dium atoms in the low-palladium loading sam-ples were in the environment of Pd_h. According to the characterization results shown in Table 3, Pd_h atoms are sensitive to hydrogen chemisorp-tion but insensitive to oxygen chemisorption at room temperature. The oxidation product of these palladium atoms at 773 K has a Pd_hO stoichiometry.

3.2. Calorimetric measurement

Fig. 5 summarizes heat evolved $[-Q_{ox}$ in kJ $(mol\ O_2)^{-1}]$ upon oxidation of different palla-dium samples with oxygen. The observed heat also varied with the palladium loading and the oxidation temperature. For each sample, the heat of oxidation displayed a plateau value at $T < 300$ K when the oxidation was limited at the surface of palladium crystallites. However, when in-creasing the extent of oxidation, the heat of oxidation gradually decreased to a plain value. The plateau value was the heat of oxygen ad-sorption $(-Q_{ad})$ and the plain value may be considered as $-\Delta_f H$ (PdO or PdO_2), i.e., the enthalpy of palladium oxide formation.

Fig. 6 correlates the $-Q_{ad}$ measured from TG-DSC with the average diameter (d) of palla-dium crystallites. The heat evolved upon oxy-gen adsorption decreases with d according to

$$-Q_{ad}\left[kJ\ (mol\ O_2)^{-1}\right] = 373 - 14d\ (nm), \tag{5}$$

The evolved heat of adsorption increased about 100 kJ $(mol\ O_2)^{-1}$ as the size of palladium
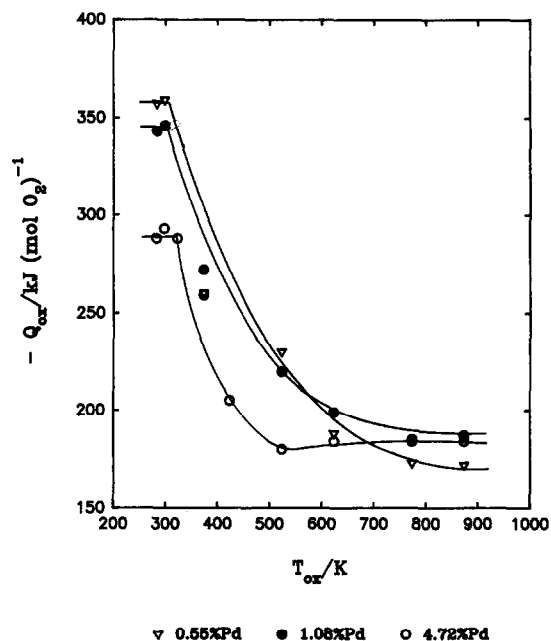
Fig. 5. Variation of the temperature profile of the heat of oxida-tion (Q_{ox}) with palladium loading on Pd/Al_2O_3 ($\triangledown$: 0.55%; $\bullet$: 1.08%; $\bigcirc$: 4.72%).

crystallites decreased from 8.0 nm to 1.5 nm (Table 3). A decreasing of $-Q_{ad}$ with the size of palladium crystallites has been previously
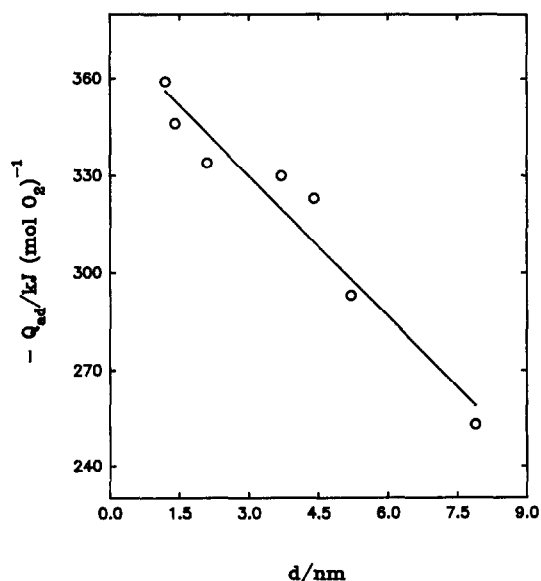
Fig. 6. Variation of Q_{ad} with the average diameter of palladium crystallites.

noted by Zakumbaeva et al. [19] and Vannice et al. [20]

The observed increase in $-Q_{ad}$ with the diameter of palladium can be attributed to changes in the electronic structure. Baetzold et al. [27] proposed, according to a theoretical calculation, that the d bandwidth of palladium crystallites increases with their particle size. With photoelectron spectroscopy, Takasu et al. [28] observed a variation in the binding energy (E_B) and the line width of core level electrons with the particle size. From X-ray absorption spectroscopy, Mason [29] also found that d-orbital vacancies of small palladium clusters increased with the palladium dispersion.

With an exception of the 0.55% Pd/Al$_2$O$_3$ (in which a significant amount of Pd$_h$O was formed upon oxidation), the $\Delta_f H(PdO)$ value measured in this study did not vary with the palladium diameter and showed a consistent value of -186 ± 2 kJ (mol O$_2$)$^{-1}$ upon oxidation at 800 K. When considering $\Delta_f H^\circ_{298} = \Delta_f H(T) + \Delta C_p(298 - T)$, a $\Delta_f H^\circ_{298} = -187$ kJ (mol O$_2$)$^{-1}$ was suggested. This value fairly correlates with the two low values (~ -173 kJ mol^{-1}) listed in Table 1 from calorimetric studies. However, this same value deviates considerably from the values (~ -220 kJ mol^{-1}) reported from the Clausius–Clapeyron method in which the variation of oxygen vapor pressure (P) over the PdO sample was related to the temperature according to

$$\mathrm{d}\ln P / \mathrm{d}T^{-1} = \Delta_f H / R. \qquad (6)$$

In this Clausius–Clapeyron method, a negligible variation of $\Delta_f H$ with the extent of oxygen desorption was assumed. However the relation $-Q_{ox} > -\Delta_f H$ is always found in Fig. 5 when Pd was only partially oxidized. The $\Delta_f H^\circ_{298}$ values calculated from Eq. (6) for PdO, therefore, should have an inherent error because a partial desorption of oxygen from sublayer PdO is required in the measurement. We believe that $\Delta_f H^\circ_{298}(PdO) = -187$ kJ (mol O$_2$)$^{-1}$, obtained in this study, is a reliable thermodynamic value. This value is highly recommended for the

$\Delta_f H^\circ_{298}(PdO)$ for future editions of physical–chemical handbooks (see the last two values in Table 1).

4. Conclusions

A commercial TG-DSC simultaneous system was successfully used in this study to investigate the phenomena of oxidation of palladium crystallites supported on alumina with O$_2$, thereby yielding the following results:

1. According to the oxygen uptake's temperature profile, the oxidation proceeded in three consecutive steps, i.e., surface adsorption ($T < 300$ K), penetration of oxygen into the sublayer (300–800 K) and complete bulk oxide formation ($T > 800$ K).

2. The heat of surface adsorption decreased with an increase in the size of palladium crystallites according to an empirical relation of

$$-Q_{ad} \left[kJ \, (mol \, O_2)^{-1} \right] = 373 - 14d \, (nm).$$

3. The product of bulk oxidation depended on the size of palladium crystallites. PdO or PdO$_2$ was formed by 773 K oxidation for large crystallites and small crystallites, respectively. The $\Delta_f H^\circ_{298}(PdO)$ was -187 ± 2 kJ (mol O$_2$)$^{-1}$ and did not vary significantly with the particle size of the palladium crystallites.

4. Nevertheless, the heat of Pd oxidation varies with the extent of oxidation. Consequently, the $\Delta_f H^\circ_{298}(PdO)$ values reported in the literature from the Clausius–Clapeyron equation should have a systematic error because oxygen ions in the sublayers of PdO have already partially desorbed upon measurements.

References

[1] R.J. Wu, T.Y. Chou and C.T. Yeh, Appl. Catal. B, 6 (1995) 105.

[2] J.-W. He, U. Memmert and P.R. Norton, J. Chem. Phys. 90 (1989) 5088.

[3] M. Milum and P. Pervan, Surf. Sci. 218 (1989) 363.

[4] T. Paryjczak, W.K. Jozwiak and J. Goralski, J. Chromatogr. 155 (1978) 9.

[5] L. Wohler, Z. Elektrochem. 11 (1905) 836.

[6] R. Schenck and F. Kurzen, Z. Anorg. Allg. Chem. 220 (1934) 97.

[7] L. Wohler and N. Jockum, Z. Phys. Chem. A 167 (1933) 169.

[8] W.E. Bell, R.E. Inyard and M. Tagami, J. Phys. Chem. 70 (1966) 3735.

[9] G. Bayer and H.G. Wiedemann, Thermochim. Acta, 11 (1975) 79.

[10] L. Brewer, Chem. Rev. 52 (1953) 1.

[11] J.B. Pedley and E.M. Marshall, J. Phys. Chem. Ref. Data 12 (1983) 982.

[12] D.R. Lide, Handbook of Chemistry and Physics, 72nd Ed. (1991–1992) pp. 5–44.

[13] H. Conrad, G. Ertl, J. Kuppers and E.E. Latta, Surf. Sci. 65 (1977) 245.

[14] G. Ertl and J. Koch, Z. Phys. Chem. N. F. 69 (1970) 323.

[15] G. Ertl and P. Rau, Surf. Sci. 15 (1969) 443.

[16] M.H. Bortner and G. Parravano, Adv. Catal. 9 (1957) 424.

[17] D. Brennan, D.O. Hayward and B.M.W. Trapnell, Proc. Roy. Soc. London Ser. A. 256 (1960) 81.

[18] G. Ertl and J. Koch, in: 5th Int. Congr. Catal. (1972) p. 969.

[19] G.D. Zakumbaeva, N.A. Azkarina, V.A. Naidin, A.M. Dostiyarov, N.F. Toktabaeya and E.N. Litvyakova, Kinet. Katal. 24 (1983) 379.

[20] P. Chou and M.A. Vannice, J. Catal. 105 (1987) 342.

[21] N.E. Buyanova, N.B. Ibragimova, A.P. Karnaukhov and N.G. Koroleva, Kinet. Katal. 13 (1972) 1295.

[22] Y.L. Lam and M. Boudart, J. Catal. 47 (1977) 393.

[23] G. Chen, W.T. Chou and C.T. Yeh, Appl. Catal. 8 (1983) 389.

[24] Y.S. Ho, Ph.D. thesis, National Tsinghua University (1990) ch. 5.

[25] I.S. Shaplygin, G.L. Aparnikov and V.B. Lazarev, Russ. J. Inorg. Chem. 23 (1978) 488.

[26] R.W. McCabe, C. Wang and H.S. Woo, J. Catal. 114 (1988) 354.

[27] R.C. Baetzold, M.G. Mason and J.F. Hamilton, J. Chem. Phys. 72 (1980) 366.

[28] Y. Takasu, R. Unwin, B. Tesche and A.M. Bradshaw, Surf. Sci. 77 (1978) 219.

[29] M.G. Mason, Phys. Rev. B 27 (1983) 748.